The role of rhizosphere in enhancing N availability in a mature temperate forest under elevated CO_2

Manon Rumeau [a,b,*], Fotis Sgouridis [d], Rob MacKenzie [a,b], Yolima Carrillo [c], Michaela K. Reay [e], Ian P. Hartley [f], Sami Ullah [a,b,**]

[a] *Birmingham Institute of Forest Research, University of Birmingham, Birmingham, UK*
[b] *School of Geography, Earth and Environmental Science, University of Birmingham, Birmingham, UK*
[c] *Hawkesbury Institute for the Environment (HIE), Western Sydney University Richmond, Australia*
[d] *School of Geographical Sciences, University of Bristol, Bristol, UK*
[e] *Organic Geochemistry Unit, School of Chemistry, University of Bristol, UK*
[f] *Geography, Faculty of Science, Environment and Economy, University of Exeter, Exeter, UK*

ARTICLE INFO

ABSTRACT

Enhanced growth of trees under elevated atmospheric CO_2 concentration ('CO_2 fertilisation') can potentially reduce a fraction of anthropogenic CO_2 emissions but is anticipated to become progressively constrained by nitrogen (N) limitation in temperate ecosystems. However, it is believed that this constraint may be mitigated if trees under elevated CO_2 (eCO_2) prime microbial activity in their rhizosphere to release available N. We assessed whether mature trees under eCO_2 regulate N availability in their rhizosphere to meet increased N demand. We hypothesized that eCO_2 primes N mineralization in the rhizosphere while reducing N losses through nitrification and denitrification. This study was conducted in a mature English-Oak-dominated temperate forest in central England, in the sixth year of Free Air CO_2 Enrichment (FACE). In the summer of 2022, we measured N transformations, enzyme activities, and nutrient pools in the rhizosphere and bulk soil of the organic layer (0–7 cm) under laboratory conditions. While the rhizosphere was found to be inherently more active (i.e. positive N priming) than the bulk soil, the effect of eCO_2 were not consistently stronger in the rhizosphere. Available soil N, dissolved organic carbon and microbial biomass were enhanced under eCO_2 in bulk and rhizosphere soils. Net N mineralization was enhanced under eCO_2 in the bulk and rhizosphere soils while leucine aminopeptidase activity, associated with organic N depolymerization, was enhanced solely in the rhizosphere. Despite higher C and N availability creating potential hot spots, nitrification was reduced under eCO_2 and denitrification remained unaffected in the rhizosphere, demonstrating a more efficient conservation of N under eCO_2. Our findings demonstrate that eCO_2 stimulates N-mining and reduce N losses in the rhizosphere. Furthermore, the tenfold difference in N turnover rates between rhizosphere and bulk soils suggests that expanding rhizosphere mass from increased root biomass may help trees under eCO_2 to meet higher N demand.

1. Introduction

Temperate forests under elevated atmospheric CO_2 (eCO_2) concentration are expected to require more available nitrogen (N) to be able to sustain the higher net primary productivity (NPP) triggered by the CO_2 fertilisation effect (Gardner et al., 2021; Norby et al., 2002). Biogeochemical simulations and meta-analysis indicate that enhanced photosynthesis under eCO_2 exacerbates progressive N limitation (PNL) of forest ecosystems because more N will be sequestered in long lasting biomass pools (De Graff et al., 2006; Johnson, 2006; Luo et al., 2004; McMurtrie et al., 2008; van Groenigen et al., 2006). This hypothesis was supported by one of the firsts free air carbon enrichment (FACE) experiments involving young sweetgum plantation at Oak Ridge FACE, where the initially enhanced NPP decreased after a few years of eCO_2 treatment, indicating N limitation of the growth enhancement (Norby et al., 2010). However, outcomes from a similar FACE experiment (Duke FACE) challenged the PNL hypothesis as enhanced NPP was maintained over 11 years, suggesting N supply in soils was sustained via enhanced

decomposition of soil organic matter (SOM) (Phillips et al., 2011). This discrepancy between CO_2 manipulation experiments demonstrates our lack of understanding in forest N cycling, especially in the context of climate change and rising atmospheric CO_2 (U.S. DOE, 2020). Furthermore, while most FACE experiments have been conducted in systems with young trees (Norby and Zak, 2011), recent observations in a mature forest (EucFACE) showing lower-than-expected C uptake responses to eCO_2 challenged original thinking on whether mature trees can initiate an enhancement of photosynthesis under eCO_2 (Jiang et al., 2020; Pihlblad et al., 2023). Thereby, it is uncertain whether the way trees regulate biochemical cycles under eCO_2 is similar in mature forests which had decades to interact with soil microbial communities and exhaust soil nutrient resources (Norby et al., 1999).

Tree ability to enhance N availability is largely governed by their interactions with microbes. For instance, under eCO_2, trees in association with ectomycorrhizal fungi (ECM) can acquire N at low cost due to the fungi's ability to access SOM (Pellitier et al., 2021; Stuart and Plett, 2020; Terrer et al., 2018). More generally, plant-microbe interactions in the rhizosphere have been identified as a key mechanism for increasing N supply to plants under eCO_2 (Meier et al., 2015; Phillips et al., 2011, 2012). However, rhizosphere priming effect (RPE) defined as the stimulation or retardation of SOM decomposition by root presence and exudation (Carrillo et al., 2014; Dijkstra et al., 2013), can both increases or decreases N availability depending on soil nutrient status, soil and/or exudate C:N ratio and microbial nutrient acquisition strategy (Craine et al., 2007; Gaudel et al., 2024; Kuzyakov, 2002); properties likely to be affected by eCO_2. Especially, changes in root exudate composition and quantity observed under eCO_2 (Dong et al., 2021; Johansson et al., 2009; Phillips et al., 2009) are likely to enhance SOM decomposition to meet the higher tree nutrient demands (Meier et al., 2015; Pihlblad et al., 2023; Terrer et al., 2021). For instance, enhanced exudation of dissolved organic carbon was found to stimulate microbial activity and therefore the secretion of N-acquiring enzymes in low-N soils (Phillips et al., 2011). Organic acids were also found to be released in higher quantity under eCO_2 (Hasegawa et al., 2023), which could directly destabilize SOM and mobilise nutrients into bioavailable forms (Jilling et al., 2018).

However, enhanced SOM decomposition for N release could progressively lead to a depletion of soil C pools, offsetting the biomass C sink under eCO_2 (Terrer et al., 2021). This soil-for-plant C offsetting may be especially significant if slow cycling pools of SOM are targeted, as it has been observed by the gradual reduction of mineral associated organic matter (MAOM) pool under eCO_2 (Dorodnikov et al., 2011; Hofmockel et al., 2011) or by the loss of *old C* (Carrillo et al., 2018). Enzyme activity can provide valuable insights into which specific pools of soil organic matter (SOM) are being targeted for decomposition under eCO_2. A shift between oxidative and hydrolytic enzyme activity can indicate which components of SOM are primed, since oxidative enzymes often initiate the first step of complex organic matter break-down or destabilization (Jilling et al., 2018). eCO_2 was found to promote hydrolytic over oxidative enzyme activity indicating a preference for decomposing simple molecules (Xiao et al., 2018), this preference reversed over time at Duke FACE (Finzi et al., 2006b). Therefore, how eCO_2 influences rhizosphere priming and its subsequent impact on soil C pools over time remains uncertain (Hyvönen et al., 2007; Kuzyakov et al., 2019; Terrer et al., 2021).

In addition, the regulation of N losses via dissimilatory reduction to N gases and leaching into groundwater in the rhizosphere under eCO_2 is poorly understood (Barnard et al., 2005; Rütting and Andresen, 2015). Nitrification and denitrification in the rhizosphere could be enhanced because of the higher C availability and, hence, higher microbial activity (Philippot et al., 2009) or, conversely, trees could exudate higher concentrations of biological nitrification inhibitor (BNI), as a N conservation strategy (Guyonnet et al., 2017; Jilling et al., 2018; Subbarao et al., 2007). Therefore, constraining N availability under eCO_2 requires an understanding of N turn-over and loss regulation in forest rhizosphere of mature trees as well as an understanding of microbial ecological strategies.

In this study, we aimed at understanding the response of N availability in the rhizosphere under eCO_2 in a mature deciduous forest, six years into CO_2 fumigation treatment at the Birmingham Institute of Forest Research (BIFoR) Free Air Carbon Dioxide Enrichment (FACE) facility in the UK. We assessed both potential net and gross N mineralization rates to gain comprehensive insights into the temporal changes in N availability (net mineralization measured in-situ over 28 days) and into the specific N process dynamics (gross mineralization) in the rhizosphere and bulk soils of the organic layer (0–7 cm) under elevated and ambient atmospheric CO_2 conditions after six years of fumigation treatment. We also quantified potential N_2O emissions, potential oxidative and hydrolytic extracellular enzyme activities involved in C, N and phosphorus (P) cycling to elucidate nutrient acquisition shifts. Given that eCO_2 can potentially affect exudation quantity and quality, we hypothesized that: 1) eCO_2 will prime N mineralization in the rhizosphere through the decomposition of recalcitrant SOM pools. Inversely, 2) eCO_2 will decrease nitrification and denitrification rates more strongly in the rhizosphere than in the bulk soils as a strategy to conserve N.

2. Material & methods

2.1. Experimental set up

The study was performed at the BIFoR-FACE facility, located in a mature deciduous forest in Staffordshire, UK. The forest is dominated by English oak (*Quercus robur* L.) in the upper canopy and common hazel (*Corylus avellana* L.*),* sycamore (Acer pseudoplatanus L.), and hawthorn (Crataegus monogyna Jacq.) in the understorey. The soil at site, classified as Ortic Luvisol (Hart et al., 2020), set on glacial till and is about 50 cm deep where the organic soil layer (O) of about 7–10 cm depth overlie an A horizon (15–25 cm deep) overlying the B horizon transiting into sandstone geology. The O-layer is a sandy loam (41% sand, 43% silt, 16% clay), with a pH of 3.8 and is characterized by a high root density (1 mg cm^{-3} on average, data not shown), a high organic matter (10% of C) and low bulk density (0.45 g cm^{-3}) (Hollis et al., 2021). The mineral layer (A) is also a sandy loam (39% sand, 39% silt, 22% clay), with a pH of 4.7 and a bulk density of 0.79 g cm^{-3}. More detailed soil properties for the first 15 cm can be found in Sgouridis et al. (2023).

The BIFoR-FACE facility is composed of six infrastructure arrays, three are fumigated with a target concentration of +150 ppm of CO_2 above the ambient concentration (eCO_2) and three with ambient air (aCO_2) (Fig. 1). Fumigation started in April 2017 and operated in daylight hours from budburst (~1st April) to leaf fall (~1st November).

The towers reach one to 3 m above the local canopy top in order to fumigate the forest from ground to canopy level. Air is released from the upwind quadrant of the array through vertical vent pipes (VVPs) placed on the 16 peripheral towers in each array. Performance of the system has been reported in Hart et al. (2020), showing that the system is able to deliver the target concentration precisely; the daytime CO_2 enrichment achieved during the 2022 growing season was of 135 ± 24 ppm (mean $\pm$ SD), due to intermittency in the CO_2 supply. The mean annual air temperature at the site was of 10.8 °C (sensors HMP155 (Helsinki, Finland)) and the mean annual precipitation was 1152 mm (rain gauges at site TR-525 M (Dallas, Texas)). For a detailed site description, see Hart et al. (2020).

2.2. Soil sampling

In each array, three sampling plots of 0.5 m × 0.5 m were established, each at approximately 1-m distance from different individual oak trees. On August 13th, 2022, three soil cores of 5 cm diameter comprising exclusively the organic layer (O-horizon: Oe + Oa) after removing the leaf litter (Oi) were collected per sampling plot and bulked together to make-up one sample per sampling plot before analysis. On

Fig. 1. Schematic of the BIFoR-FACE site from (Hart et al., 2020). Fumigated arrays are represented in orange and ambient arrays are in blue.

the day of the sampling, the soil surface temperature was 15 °C and the soil gravimetric moisture in the O horizon varied between 10 and 55% (Table S1). The depth of the O-horizon varied between 5 and 9 cm between sampling areas (Table S1 and Fig. S1).

Rhizosphere soil was separated from bulk soil by gently shaking the roots. Soil that remained attached to the roots after shaking was considered as the rhizosphere sample while the rest of the sample constituted the bulk soil and was sieved through a 2 mm sieve. Masses of rhizosphere and bulk soils were recorded to calculate the proportion of rhizosphere. Roots were kept and visually identified as "oak root" or "non-oak root" to determine the relative proportion of oak rhizosphere (Table S2). Rhizosphere and bulk soil samples were stored at 5 °C until further analysis.

2.3. Nutrient standing pools analysis

To determine soil nutrient pools, we quantified soil ammonium (N–NH$_4^+$), nitrate (N–NO$_3^-$), free amino acids (FAA), dissolved organic C (DOC), dissolved N (DN), microbial biomass C and N (MBC and MBN) and total C and N contents. All nutrient analyses were performed within a week after field collection. Gravimetric moisture was measured by drying 5 g of soil at 105 °C for 48 h. Soil pH was determined after mixing 3 g of soil in 30 ml of deionized water using a pH meter (SevenExcellence pH, Mettler Toledo, UK).

Soil NH$_4^+$ and NO$_3^-$ concentrations were measured by extracting 2 g of soil with 0.5 M potassium sulphate (K$_2$SO$_4$;soil: extractant ratio of 1:5 (*w/v*)). The extracts were filtered at 0.45 μm and analysed by continuous flow colorimetry (Skalar SA 3000 analyser, Netherlands). The limit of detection was 0.02 mg N L^{-1} for both NH$_4^+$ and NO$_3^-$. The concentrations were blank corrected and the relative standard deviation (RSD) calculated on quality control (QC) samples was below 2%.

Soil free amino acid (FAA) concentration was determined using the OPAME fluorescence assay described by Jones (2002) and adapted to a microplate assay by Darrouzet-Nardi et al. (2013). Briefly, 2 g of soil was extracted in 10 ml of 1 M KCl, shaken, filtered at 0.45 μm and 50 μl was added to a microplate with 100 μl of OPAME working reagent. As NH$_4^+$ reacts to fluorescence in the first hour, fluorescence was measured after 1 h of incubation when the fluorescence from reaction with NH$_4^+$ is negligible.

The soil concentration of DOC and DN was measured after extraction

with 0.5 M K$_2$SO$_4$, as described above, and extracts analysed on a TOC/TN analyser after a 10-fold dilution (Multi N/C 2100, Analytik Jena, Germany). Samples were blank corrected and the RSD was below 1% for DOC and below 4% for DN.

The dried soils used for soil moisture determination were manually pulverized with a pestle and a mortar and approximatively 8 mg was weighed in a tin capsule. These samples were analysed for total C and N soil concentrations by an elemental analyser (EA) (vario PYRO cube; Elementar Analysensysteme GmbH, Hanau, Germany). The EA was calibrated with sulphanilamide (N: 16.26%, C: 41.81%) and the precision was below 5% RSD for both C and N.

C and N in the microbial biomass (MBC and MBN) were measured according to the chloroform extraction method (Brookes et al., 1985). For each soil sample, two subsamples were weighed and one was fumigated with chloroform for 48 h. Blanks without soil were also fumigated. Fumigated and non-fumigated soil subsamples were then extracted with K$_2$SO$_4$ (0.5 M) for DOC and DN quantification as above. MBC and MBN were calculated as the difference in the DOC and DN concentrations between the fumigated and the non-fumigated samples and divided by a correction factor of 0.45.

2.4. ^{15}N isotopic pool dilution combined with the ^{15}N Gas Flux method

Gross N mineralization, nitrification rates, soil N$_2$O emissions from nitrification and denitrification were assessed by a^{15}N pool dilution method as described by Hart et al. (1994) combined with a^{15}N Gas flux method as described by Sgouridis et al. (2023) within 2 weeks of sampling.

2.4.1. Labelling and incubation

Rhizosphere soils (5 g) and bulk soils (10 g) were weighed in quadruplets into airtight specimen cups equipped with a septum on the lid to allow gas sampling. Before labelling, all samples were acclimated in the dark at 15 °C for 2 days, chosen to match the soil temperature on the sampling day. To achieve a simultaneous 20% enrichment in ^{15}N atom percentage (to avoid stimulating microbial activity) (Micucci et al., 2024) and raise the soil moisture to 35% (average of soil gravimetric moisture in summer) in all samples, various labelling solutions were prepared using K^{15}NO$_3$ (98 at. % ^{15}N, Sigma-Aldrich) or ^{15}NH$_4$Cl (98 at. % ^{15}N, Sigma-Aldrich). The labelling solutions were added dropwise,

and soils were gently stirred with a spatula to ensure a uniform distribution of labels before closing the specimen cups. Immediately after labelling and following a 24 h incubation at 15 °C in the dark, soil samples were extracted with 1 M KCl. A soil extract aliquot was analysed for extractable N–NH_4^+ and N–NO_3^-, as described above, and the rest of the soil extract was used to extract the ^{15}N content in the NH_4^+ and NO_3^- pools using the gas diffusion procedure (Davidson et al., 1991; Hart et al., 1994).

Concurrently, 20 ml of gas was sampled near the soil surface with a syringe before cup closure and transferred into a pre-evacuated 12 ml gas exetainer vial (Labco, Ceredigion, UK). A final set of gas samples were obtained after 24 h of incubation by pumping the headspace (100 ml) with a syringe through the septum and transferring into a 12 ml gas exetainer. These samples were analysed for total CO_2, N_2O and CH_4 concentration on a gas chromatograph (GC; Agilent Technologies Ltd, USA) equipped with µECD (electron capture detector) and FID (flame-ionisation detector). The ^{15}N content of the N_2O was determined using a continuous flow isotope ratio mass spectrometer (IRMS; Elementar Isoprime Precision; Elementar Analysensysteme GmbH, Hanau, Germany) coupled with a trace-gas pre-concentrator inlet with autosampler (isoFLOW GHG; Elementar Analysensysteme GmbH, Hanau, Germany). Gas samples in the 12 ml exetainer were purged into a He stream through the autosampler and then entered 2 sequential liquid N_2 traps to isolate and cryofocus the N_2O. The gas sample containing the concentrated N_2O was separated from any residual CO_2 via a GC column before passing though the IRMS where the N_2O isotopologues and R45 and R46 ratios were measured at a current of 600 µA. Ten N_2O reference samples were run before any of the samples to ensure instrument stability and a $\delta^{15}N$ standard deviation lower of 0.05‰.

2.4.2. Gas diffusion procedure on enriched soil extracts

The diffusion procedure was performed according to Davidson et al. (1991) and Hart et al. (1994). The aim is to diffuse the enriched pool of either NH_4^+ or NO_3^- onto an "acid trap" to then measure the ^{15}N at% of these N pools by an EA-IRMS (elemental analyser-IRMS: Elementar Isoprime Precision; Elementar Analysensysteme GmbH, Hanau, Germany). Acid traps were prepared with 8 mm diameter Whatman 3 filter discs soaked with 10 µL of 2.5 M $KHSO_4$ and wrapped in sealing PTFE tape. Using 20–40 ml of soil extract, NH_4^+ was diffused by simultaneously adding 0.2 g of MgO and an acid trap. To ensure complete diffusion, extracts were shaken at low speed for 7 days. Then, acid traps were retrieved, dried in a desiccator, and encapsulated in tin capsules for EA-IRMS analysis. To diffuse NO_3^-, NH_4^+ was first removed from the solution using the above procedure but the filters were discarded. NO_3^- was then diffused by adding 100 µL of 30 % Brij-35 and 0.4 g of Devarda's alloy, which reduces NO_3^- to NH_4^+. A second acid trap was placed into the specimen cups and samples were let for another 7 days at room temperature on reciprocal shaker. The filters disks were dried, wrapped and analysed for ^{15}N at% on EA-IRMS.

2.4.3. Calculations

Gross mineralization fluxes were calculated using the following equations developed by Kirkham and Bartholomew (1954):

$$M \left(\mu g\, g^{-1}\, day^{-1} \right) = \frac{[NH_4^+]_0 - [NH_4^+]_t}{t} \times \frac{\log\left(\frac{APE_0}{APE_t}\right)}{\log\left(\frac{[NH_4^+]_0}{[NH_4^+]_t}\right)} \quad (1)$$

$$C \left(\mu g\, g^{-1}\, day^{-1} \right) = M - \frac{[NH_4^+]_t - [NH_4^+]_0}{t} \quad (2)$$

Where M = gross mineralization rate, C = NH_4^+ consumption rate, t = time elapsed, $[NH_4^+]$ = NH_4^+ soil concentration (µg g^{-1}), APE_τ = ^{15}N atom percent excess of the NH_4^+ pool, τ. Gross rates of nitrification and NO_3^- consumption were calculated by replacing NH_4^+ concentration by

NO_3^- concentration, and APE in the NH_4^+ pool by the APE in the NO_3^- pool. NH_4^+ immobilization rate is equal to the difference between NH_4^+ consumption rate and gross nitrification. NO_3^- immobilization rate is assumed equivalent to the gross NO_3^- consumption rate.

Total N_2O emissions and basal respiration (i.e. CO_2 flux) were calculated using the following equation (CO_2 flux example):

$$CO_2\, flux \left(\mu gC\, g^{-1}\, h^{-1} \right) = \frac{\left([CO_2]_t - CO_2]_0 \right) \times H}{m \times t} \quad (3)$$

Where $[CO_2]_\tau$ = concentration of CO_2 in µg C L^{-1} in the vial, H = headspace in L, m = mass of dry soil (g), t = time elapsed (h). N_2O flux is calculated in the same way by substituting the concentration in N_2O in µg N L^{-1} in the above equation. N_2O from nitrification and denitrification were calculated as described in Sgouridis et al. (2023)

To assess microbial activity, the microbial metabolic quotient (qCO_2) was calculated by dividing microbial respiration by the microbial biomass C (Anderson and Domsch, 1993).

Finally, primed C and N by rhizosphere effect (Yin et al., 2021) were calculated as follows where R and B represent rhizosphere and bulk soil respectively (Equations (4) and (5)):

$$Primed\, C \left(\mu gC\, g^{-1}\, h^{-1} \right) = R_{CO_2\, flux} - B_{CO_2\, flux} \quad (4)$$

$$Primed\, N \left(\mu gN\, g^{-1}\, h^{-1} \right) = R_{gross\, mineralization} - B_{gross\, mineralization} \quad (5)$$

2.5. Enzyme assays

The activities of six soil extracellular enzymes involved in microbial C, N and P cycling were assayed. These enzymes fall into two functional groups based on the type of compounds they are able to decompose. Oxidative enzymes including peroxidase (PEROX) and phenol oxidase (PHENOX) decompose recalcitrant SOM such as lignin. Hydrolytic enzymes involved in several organic compound breakdown such as β-N-acetyl-glycosaminidase (NAG) and leucine aminopeptidase (LAP) for organic N, β-glucosidase (BG) for organic C and acid phosphatase (AP) for organic P.

2.5.1. Fluorometric assays

Hydrolytic enzymes activities were determined by fluorimetry. Within 2 weeks after sampling, soil suspensions were prepared by sonicating 2 g of soil in 125 ml of acetate buffer (pH 5.2). While stirring, 200 µl of soil suspension were added in duplicate to 50 µl of substrate solution of 200 µM (Table S2) on a sterile black 96-well microplate. Quenched standard wells received 200 µl of soil suspension and 50 µl of either 4 methylumbelliferone, or 7-amino-4-methyl coumarin at concentrations ranging from 0.025 µM to 50 µM. Reference standard wells received 50 µl of standard (same as above) and 200 µl acetate buffer. Blank wells received 50 µl of acetate buffer and 200 µl of soil suspension and negative control wells received 50 µl of substrate and 200 µl of acetate buffer. Fluorescence was measured at 30 °C every 5 min for an hour with excitation wavelength of 365 nm and an emission wavelength of 450 nm. Fluorescence intensity after the first 10 min of pre-incubation was plotted over time. The slope of the linear regression and coefficient of determination were calculated. Each regression was visually assessed, and any outliers were removed to ensure a satisfactory coefficient of determination ($R^2 > 0.97$). The slope was then used to determine the activity. An example of the linear regression can be found in Fig. S2.

2.5.2. Colorimetric assays

Phenol oxidase (PHENOX) and Peroxidase (PEROX) activities were determined by measuring absorbance at 450 nm. Soil suspensions were prepared by sonicating 0.5 g of soil in 125 ml of acetate buffer (pH 5.2). Again, 200 µl of soil suspension were added to 50 µl of substrate solution (25 mM DOPA) (Table S2) on a sterile transparent 96-well microplate. For peroxidase assays, 10 µl of 0.3 % H_2O_2 was added to the 50 µl of 25

mM DOPA substrate. Blank wells received 50 μl of acetate buffer and 200 μl of soil suspension, negative control wells received 200 μl of acetate buffer and 50 μl of substrate solution (+10 μl of 0.3% H_2O_2 in the case of Peroxidase). Absorbance was measured at 30 °C every 5 min for 2 h for Peroxidase, and every few hours for up to 48 h for Phenol oxidase. Similarly, activity was calculated as the slope of absorbance over time.

2.5.3. Calculations of microbial carbon use efficiency (CUE) and nitrogen use efficiency (NUE) from enzyme activities

We calculated microbial CUE and NUE (e.g. amount of nutrient assimilated in microbial cells over the amount taken up) from the elemental stoichiometry of organic matter and microbial biomass, and the ratios of C to N-acquiring eco-enzymatic activities (Sinsabaugh et al., 2016) (Equations (6) and (7)). This method assesses how microbes shift their resource use efficiency in response to substrate stoichiometry (Schimel et al., 2022).

$$CUE_{C:N} = CUE_{max}\left(\frac{S_{C:N}}{(S_{C:N}+K)}\right) \quad where\ S_{C:N} = \frac{1}{EEA_{C:N}} \times \frac{B_{C:N}}{L_{C:N}} \tag{6}$$

$$NUE_{N:C} = NUE_{max}\left(\frac{S_{N:C}}{S_{N:C}+K}\right) \quad where\ S_{N:C} = (1 - EEA_{N:C}) \times \frac{B_{N:C}}{L_{N:C}} \tag{7}$$

where $S_{C:N}$ is a scalar that quantifies how ecoenzymatic activities allocate resources to mitigate differences between the elemental composition of available resources and that of microbial biomass. CUE_{max} is set at 0.6, NUE_{max} is set at 1.0 and K is the half saturation constant set at 0.5 (Sinsabaugh et al., 2016). $EEA_{C:N}$ refers to the enzymatic C:N ratio, $B_{C:N}$ is the microbial C:N ratio and $L_{C:N}$ is the soil DOC:DN ratio.

2.6. Net N mineralization

Nitrogen net mineralization rates were measured in June 2022 and August 2022. On June 6th and August 2nd, 5 replicates of organic soils (O horizon) were collected per array. On the same day, the rhizosphere soil was separated from the bulk soil as described above. Each bulk and rhizosphere sample were divided into two subsamples; one subsample was left for 28 d incubation in a polyethylene bag buried in-situ under the leaf litter (T28d) and the other (T0) was transported to the laboratory and analysed for extractable $N–NH_4^+$ and $N–NO_3^-$ (see method description above). After 28 days, incubated T28d samples were retrieved and analysed for extractable $N–NH_4^+$ and $N–NO_3^-$. Net mineralization and net nitrification were then calculated as the difference $N–NH_4^+$ and $N–NO_3^-$ content between the T0 and the T28d samples.

2.7. Statistical analyses

Statistical analyses were carried out with Rstudio software (version 3.6.1) (R Core Team, 2017). Linear mixed effect models were used to evaluate soil fraction (rhizosphere or bulk soil) and treatment (eCO_2 or aCO_2) effects, with soil fraction and treatment set as fixed effects, and array set as random effects ("lmer" function, lme4 package (Bates et al., 2015)). Due to high variability and low number of replications in FACE experiment (n = 3) we considered that a p-value (p) between 0.1 and 0.05 indicates an effect and a p-value <0.05 indicates a significant effect. A Tukey's multi-comparison test was performed when the treatments or soil fraction had a significant effect on the variable ($p < 0.05$). Furthermore, to detect treatment effect independently from the soil fraction, one-way ANOVA models were performed on the rhizosphere data and on the bulk soil data separately (Table S3). When the assumptions of normality and homogeneity of variance were not met, log transformations were performed to meet model assumptions (Table S3). Correlations between variables were assessed using Pearson correlation tests and R-squared coefficients of determination. To estimate the eCO_2 effect, we calculated the natural log of the response ratio (RR) as an effect size and its corresponding pooled variance (V) (Hedges et al.,

1999) between the eCO_2 and aCO_2 treatment in both the bulk soil and the rhizosphere soil separately (Equations (8) and (9)).

$$lnRR = \ln\left(\frac{Xe}{Xa}\right) \tag{8}$$

$$V = \frac{Se^2}{(Ne \times Xe^2)} + \frac{Sa^2}{(Na \times Xa^2)} \tag{9}$$

where X_e and X_a are the mean values of a specific variable in the eCO_2 and aCO_2 treatment respectively; N_e and N_a are the sample sizes; and S_e and S_a are the standard deviations.

3. Results

3.1. Soil nutrient standing pools

Expect of NO_3^-, all nutrient pools showed a positive rhizosphere effect with notably NH_4^+ increasing by 100%, DOC by 13%, free amino acids (FAA) by 18% and C:N ratio by 7% relative to the bulk soil ($p < 0.05$) (Table 1, Fig. S3). Soil total C, N and microbial biomass pools were also higher, though the difference was not significant ($p > 0.05$). Soil NH_4^+ concentration, dissolved organic carbon (DOC) concentration and dissolved nitrogen (DN) were significantly higher under eCO_2 in both rhizosphere and bulk soils while FAA and NO_3^- concentrations remained unaffected by eCO_2 (Table 1). MBC was also higher under eCO_2 in both bulk and rhizosphere soils while MBN only increased significantly in the bulk soil (Table 1). Consequently, the microbial C:N ratio was increased by 10% under eCO_2 in the rhizosphere ($p > 0.05$). Total C and N were higher under eCO_2 in the bulk soil but lower in the rhizosphere ($p > 0.05$). Overall, most soil nutrient and microbial biomass pools were positively affected by eCO_2 but displayed a stronger eCO_2 effect in the bulk soil ($lnRR_{bulk-pool} = 0.32$ on average against $lnRR_{rhizosphere-pool} = 0.08$) (Fig. 2). Additionally, while the difference was not significant, the relative proportion of rhizosphere soil was slightly higher under eCO_2 (23.7%) compared to aCO_2 (21.2%) (Fig. 3C).

3.2. Nitrogen and carbon fluxes

3.2.1. Nitrogen mineralization and nitrification

Gross and net mineralization rates were ten times higher in the rhizosphere compared to bulk soils (Fig. 3). However, while eCO_2 had no discernible impact on gross rates or on the amount of primed N (Table 2), it increased net rates in both bulk and rhizosphere soils (RR > 0.9) (Fig. 2), but this enhancement was only significant in the rhizosphere (+150% in August) (Fig. 3B). Gross nitrification and net nitrification were both enhanced in the rhizosphere but only under aCO_2 ($p < 0.05$). Consequently, nitrification was lower under eCO_2 compared to aCO_2 in the rhizosphere ($p > 0.05$) (Fig. 3), this reduction was especially pronounced on the gross rates (RR = − 0.80) compared to the net rates (RR = − 0.25) (Fig. 2). Additionally, gross nitrification showed a positive correlation with soil DOC and DN content under aCO_2 but not under eCO_2 (Fig. S4) while net nitrification was mostly correlated with soil moisture (Fig. S5). Finally, while gross and net mineralization rates were positively correlated ($R^2 = 0.30$), gross and net nitrification showed a poor correlation ($R^2 = 0.03$) (Fig. S6).

NH_4^+ and NO_3^- consumption mirrored the production rates, showing no effect of eCO_2 on NH_4^+ consumption but indicating lower NO_3^- consumption in the rhizosphere (Fig. 3A). NO_3^- immobilization by microbes can be approximated by NO_3^- consumption, given that N_2O emission by denitrification is comparatively minimal. NH_4^+ immobilization, approximated by the difference between NH_4^+ consumption and gross nitrification, was higher in the rhizosphere ($8.4 \pm 13.3\ \mu g\ g^{-1}\ d^{-1}$) ($p > 0.05$) compared to the bulk soil where NH_4^+ immobilization was barely detectable ($0.3 \pm 1.2\ \mu g\ g^{-1}\ d^{-1}$). NH_4^+ and NO_3^- mean residence times (MRT) were calculated as the nutrient pool divided by the rate of

Table 1
Soil nutrient content and microbial biomass in bulk soil and rhizosphere soil under aCO$_2$ (ambient) and eCO$_2$ (elevated) and ANOVA test results with p-value below 0.1 highlighted in bold. Mean values and standard errors are indicated for each soil fraction and treatment (n = 9).

	Bulk soil		Rhizosphere soil		ANOVA p-value		
	aCO$_2$	eCO$_2$	aCO$_2$	eCO$_2$	*fraction*	*treatment*	*fraction x treatment*
Gravimetric moisture (%)	22 ± 3	25 ± 5	21 ± 3	21 ± 4	**0.08**	0.83	0.48
pH	3.9 ± 0.2	3.8 ± 0.2	3.8 ± 0.1	3.9 ± 0.2	0.77	0.83	0.21
N–NO$_3$ (µg g^{-1})	15 ± 5	20 ± 7	11 ± 3	13 ± 5	0.15	0.52	0.15
N–NH$_4^+$ (µg g^{-1})	3.8 ± 0.7	6.9 ± 1.1	9.5 ± 2.2	11.4 ± 1.4	**<0.001**	**<0.001**	0.24
N-FAA (µg g^{-1})	2.8 ± 0.2	3.3 ± 0.4	3.4 ± 0.3	3.8 ± 0.3	**0.06**	0.44	0.88
MBC (µg g^{-1})	695 ± 62	969 ± 79	791 ± 91	914 ± 93	0.69	**0.02**	0.36
MBN (µg g^{-1})	86 ± 7	119 ± 10	100 ± 13	106 ± 13	0.85	0.45	**0.08**
MBC:MBN ratio	8.1 ± 0.2	8.2 ± 0.3	8.1 ± 0.3	8.9 ± 0.3	0.23	0.42	0.18
DOC (µg g^{-1})	240 ± 11	311 ± 25	284 ± 7	333 ± 19	**0.05**	**0.06**	0.52
DN (µg g^{-1})	33 ± 4	44 ± 8	38 ± 4	43 ± 3	0.18	**0.03**	0.50
Total C (%)	8.9 ± 1.7	13.0 ± 2.3	13.3 ± 2.5	10.9 ± 1.6	0.57	0.7	**0.10**
Total N (%)	0.50 ± 0.07	0.67 ± 0.10	0.63 ± 0.12	0.56 ± 0.07	0.92	0.57	0.19
C:N ratio	17.1 ± 0.7	18.5 ± 0.8	19.6 ± 0.6	18.9 ± 0.5	**0.03**	0.54	**0.09**

mineralization or nitrification respectively. NH$_4^+$ MRT was 3 d in the bulk soil and 0.5 d in the rhizosphere. NO$_3^-$ MRT was faster in the rhizosphere under aCO$_2$ (from 2 d in the bulk soil to 0.7 d in the rhizosphere), but remained the same between bulk and rhizosphere under eCO$_2$.

3.2.2. N$_2$O losses by nitrification and denitrification

Under equal soil moisture, total nitrous oxide emissions were higher under eCO$_2$ in the bulk soil ($p > 0.05$) but not in the rhizosphere (Fig. 4). This enhancement was mainly explained by a higher denitrification activity under eCO$_2$ in the bulk soil ($p = 0.03$). N$_2$O emissions from nitrification were not affected by treatments in neither bulk nor rhizosphere soil. Moreover, N$_2$O emissions were positively correlated with soil MBC in the bulk soil, whereas this correlation was less pronounced in the rhizosphere (Fig. 4B). On average, denitrification and nitrification contributed to approximately 40% and 50% of the total N$_2$O emissions, respectively, leaving only 10% for other sources or errors. However, this distribution varied considerably among treatments and soil fractions. In the bulk soil, N$_2$O emissions were predominantly associated with nitrification, whereas in the rhizosphere, the primary source of N$_2$O emissions was denitrification (Fig. 4A).

3.2.3. Microbial carbon respiration

Microbial respiration was influenced by soil fraction and eCO$_2$ treatment (Table 3), but the eCO$_2$ effect was stronger in the bulk soil (RR = 0.34) compared to the rhizosphere soil (RR = 0.14) leading to no overall effect of eCO$_2$ on the positive priming effect regarding C (Table 2). The microbial metabolic quotient (qCO_2), providing insight into microbial activity was significantly higher in the rhizosphere ($p < 0.05$), with no significant enhancement under eCO$_2$ (Table 3).

3.3. Soil enzyme activities and stoichiometries

eCO$_2$ had a stronger effect on potential soil enzyme activity in the rhizosphere while trends were less noticeable in the bulk soil. Notably, in the rhizosphere, LAP was significantly enhanced under eCO$_2$ (+67%), while phenol oxidase activity was downregulated (−34%). BG activity also showed a slight enhancement in both bulk and rhizosphere soils under eCO$_2$ ($p > 0.05$) (Fig. 5). Despite these changes, microbial CUE, NUE and enzymatic ratios remained unaffected by soil fraction or eCO$_2$ (Table S4). The ratio of ln (BG):ln (PHENOX) was 14% higher under eCO$_2$ in the rhizosphere ($p = 0.12$) (Table S4) suggesting that there was a shift in the type of enzyme utilized under eCO$_2$ in the rhizosphere from oxidative to hydrolytic. The activities of all the hydrolytic enzymes (LAP, BG, NAG, AP) were positively correlated with each other, and BG especially was positively correlated with gross mineralization and NH$_4^+$ consumption (Fig. S7). Phenol oxidase activity, on the other hand, showed a negative correlation with NH$_4^+$ consumption, gross

mineralization, gross nitrification and NH$_4^+$ content (Fig. S7).

4. Discussion

Nitrogen availability and cycling were enhanced by eCO$_2$ in the bulk soil and in the rhizosphere as evidenced by the higher net mineralization rates, higher NH$_4^+$ content and higher LAP activity under eCO$_2$. The increase of the LAP enzyme activity under eCO$_2$ in the rhizosphere indicated a potential increase of protein depolymerization activity, as LAP degrades mostly proteins and peptides (Matsui et al., 2006). Higher N-acquiring enzyme production, together with the higher microbial C:N ratio observed in the rhizosphere suggests that higher C availability (i.e. DOC) under eCO$_2$ triggered a microbial N demand in the rhizosphere (Manzoni et al., 2021; Moorhead et al., 2013). Furthermore, the higher microbial respiration supports the hypothesis of a faster SOM decomposition for N-mining, resulting in increasing NH$_4^+$ availability. These findings align with studies on young tree plantations suggesting an enhanced N-mining under eCO$_2$ based on higher N-acquiring enzyme activities (Meier et al., 2015; Phillips et al., 2011) or net mineralization (Finzi et al., 2002, 2006a). However, only few studies have detected signs of gross mineralization enhancement (i.e. prime indicator of N-mining) (Phillips et al., 2011; Sgouridis et al., 2023), indicating that it may only be discernible in highly N-limited systems (Andresen et al., 2020; Rütting and Andresen, 2015). Therefore, net rates, measured *in-situ* on long term incubation periods, may be more sensitive to changes in N availability changes compared to gross rates (Verchot et al., 2001). Yet, further evidence is required to confirm whether the increased net mineralization results from higher SOM decomposition and not only from lower NH$_4^+$ consumption. Nevertheless, this experiment suggests that after six years of eCO$_2$ treatment, N availability is not constrained under eCO$_2$, as NH$_4^+$ is more available, likely due to increased SOM decomposition, as supported by higher LAP activity, net mineralization and microbial respiration.

Net nitrification and gross nitrification were slightly downregulated under eCO$_2$ in the rhizosphere despite the positive rhizosphere effect and eCO$_2$ effect creating hot spots for heterotrophic nitrification (i.e. high DOC and DN content) (Zhang et al., 2019). While high soil DOC can reduce autotrophic nitrification by promoting heterotrophic activity (Strauss and Lamberti, 2002), in acidic forest soils, heterotrophic nitrification primarily dominates (Li et al., 2018). Hence nitrification was expected to be stimulated by both rhizosphere and eCO$_2$ effects. Yet, a positive rhizosphere effect solely occurred under aCO$_2$ where rhizosphere DOC and DN levels drove increased nitrification activity. This suggests that another mechanism is involved in the reduction of nitrification under eCO$_2$. Earlier research on bulk soils has generated inconsistent results on nitrification (Barnard et al., 2005; Rütting and Andresen, 2015; Sgouridis et al., 2023), generally pointing towards an overall lack of effect. However, a decrease was observed in some cases
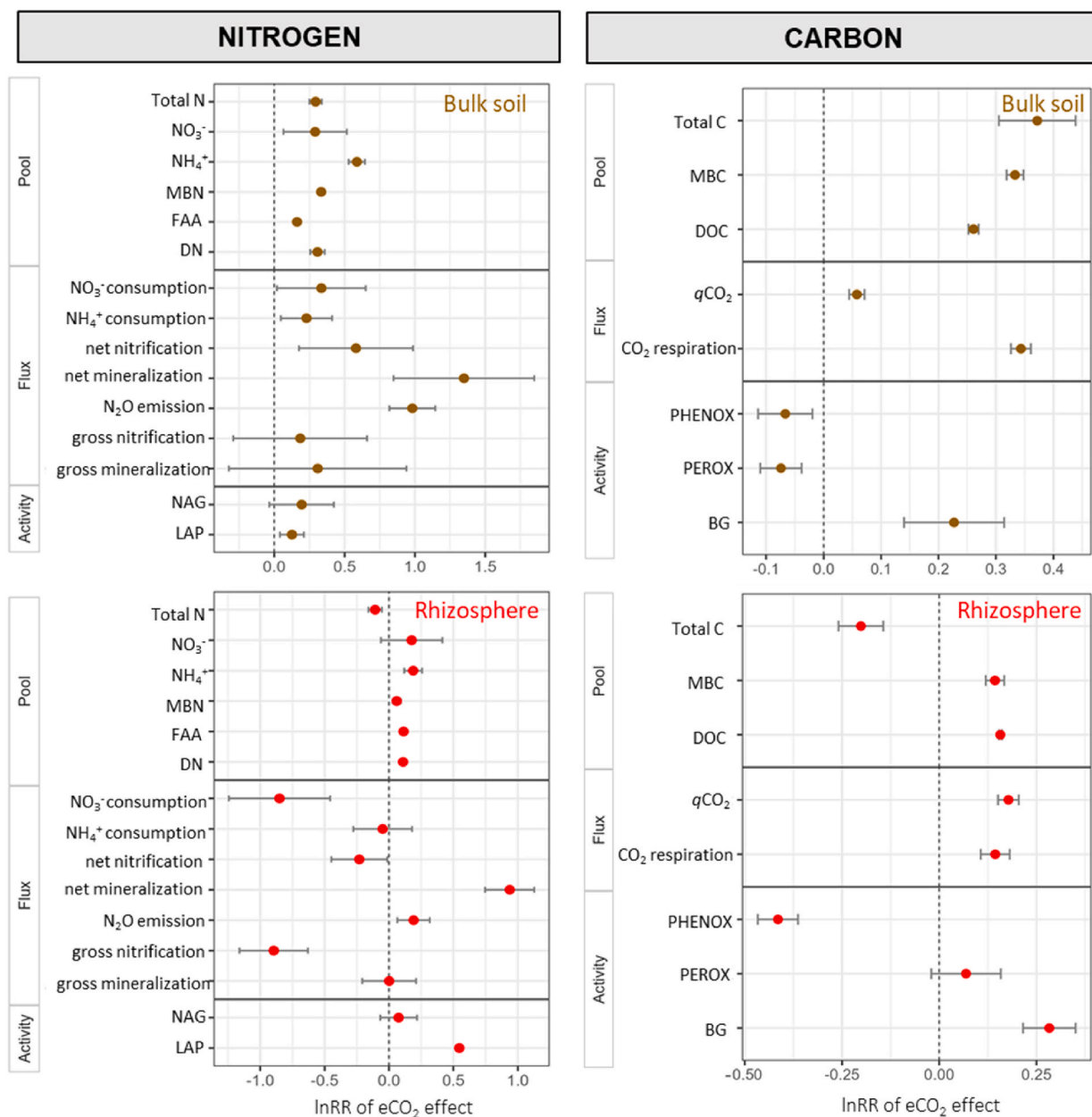
Fig. 2. Response ratio (lnRR mean with standard error) of the eCO_2 effect in the bulk (brown) and rhizosphere soil (red) relative to aCO_2 calculated for each variable (gross rates, N_2O emissions and CO_2 respiration are measured from soil incubated with 15 N label). A negative response ratio means that eCO_2 decreased that specific variable and a positive value means that eCO_2 increased that variable.

(Barnard et al., 2005; Rütting and Andresen, 2015), aligning with our observations in the rhizosphere. Nitrification can be downregulated in soils in the presence of roots either due to competition for NH_4^+ (Dijkstra et al., 2013; Zhu et al., 2021) or due to the release of biological nitrification inhibitor (BNI) compounds by roots as a strategy to conserve N (Subbarao et al., 2007) suggesting that eCO_2 increased the competition between roots and nitrifying bacteria and may alter the concentration of BNI released by roots. Similar mechanisms may have regulated N_2O losses by denitrification in the rhizosphere (Fender et al., 2013). Denitrification was only primed by the higher C in the bulk soil while no eCO_2 effect was detected in the rhizosphere where a higher N demand by trees may have suppressed denitrifying communities (Rummel et al., 2021) and counteracted the C exudation effect. These results collectively suggest that N losses via nitrification and denitrification are reduced under eCO_2 in the rhizosphere, thereby conserving available N for tree uptake. However, further investigation is needed to understand the

underlying mechanisms of this downregulation.

Furthermore, shifts in soil enzyme activities observed in the rhizosphere indicate that the higher N-mining activity under eCO_2 primarily targets easily accessible SOM, such as proteins or cellulose, rather than recalcitrant C denoted by the lower phenol activity. Similar shifts were noted in a meta-analysis but were not significant (Xiao et al., 2018) suggesting a small yet tangible effect of eCO_2. Microbes under eCO_2 might shift their nutrient acquisition strategy, acquiring N from easily accessible nutrients provided by the higher rhizodeposition under eCO_2 (Phillips et al., 2009) rather than recalcitrant SOM (Dijkstra et al., 2013). Thereby, while the decrease in phenol oxidase activity under eCO_2 may imply a promotion of C storage (Sinsabaugh, 2010), we hypothesize that the accelerated decomposition of *new carbon* could impede C accumulation under eCO_2 (Phillips et al., 2012), aligning the lower total C found in the rhizosphere and with research suggesting an overall marginal effect of eCO_2 on soil C storage (Carney et al., 2007;
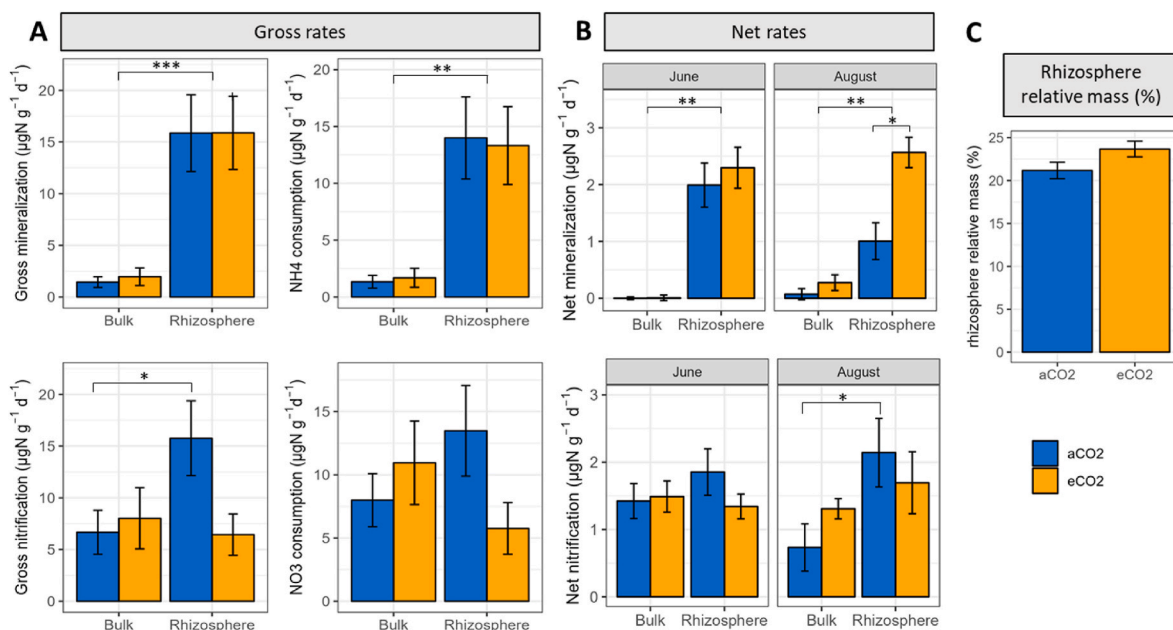
Fig. 3. Ammonium and nitrate dynamics under aCO_2 (blue) and eCO_2 (orange) in rhizosphere and bulk soils. A) Gross mineralization, gross nitrification, ammonium and nitrate consumption, where errors bars represent the standard error between replicates (n = 9) in August. B) Net mineralization and nitrification in June and August (n = 15). C) Rhizosphere relative mass expressed in percentage. Significant differences between treatments, types, or interactions are indicated with an asterisk above the respective groups.

Table 2
Primed C and N calculated as the difference in CO_2 respiration and gross mineralization respectively between rhizosphere and bulk soil (mean ± se). ANOVA results for treatment are described on the right part of the table.

Priming effect	aCO_2	eCO_2	ANOVA p-value
			treatment
Primed C	0.46	0.46	0.99
($ugC\ g^{-1}\ h^{-1}$)	±0.22	±0.32	
Primed N	16.4	14.8	0.89
($ugN\ g^{-1}\ h^{-1}$)	±6.1	±5.9	

Kuzyakov et al., 2019; Terrer et al., 2021).

While the rhizosphere was found to be inherently more *active* (i.e. positive priming of C and N) than the bulk soil, the effects of eCO_2 were not consistently stronger in the rhizosphere, contrary to our initial hypothesis. Increased nutrient availability and N mineralization were observed in both rhizosphere and bulk soils, complicating interpretations on the role of RPE on N availability under eCO_2. This could be due to the dense root distribution in the organic layer (1 mg cm^{-3}) resulting in high exudation quantity of 5 µg $cm^{-2}\ d^{-1}$ (Reay et al., *in prep*), which likely extended the priming effect into the bulk soil especially under eCO_2 where the fine root biomass is higher. Consequently,
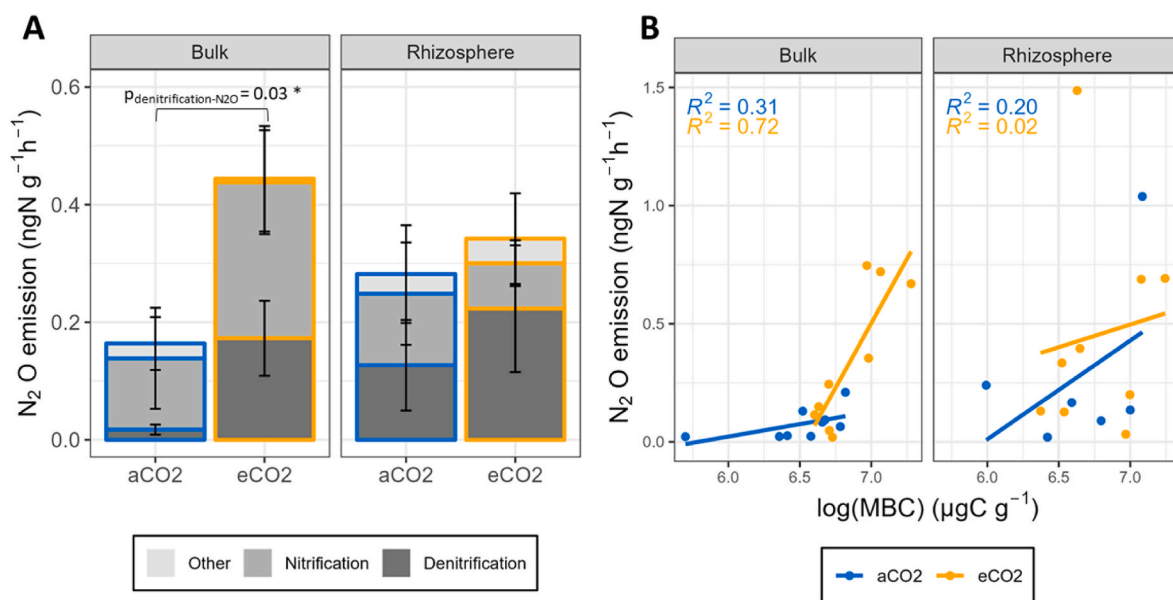
Fig. 4. A) N_2O emission source partitioned (i.e. denitrification and nitrification and other). Errors bars represent the standard error between replicates (n = 9). An asterisk indicates significant differences (p-value <0.05) between treatment for that soil fraction. B) Total N_2O emission correlation with microbial biomass carbon (MBC).

Table 3

Soil microbial respiration and microbial metabolic quotient (qCO$_2$) (mean ± se). ANOVA results for soil fraction, treatment and the interaction effects are described on the right part of the table.

Microbial respiration	Bulk soil		Rhizosphere		ANOVA p-value		
	aCO$_2$	eCO$_2$	aCO$_2$	eCO$_2$	*fraction*	*treatment*	*fraction x treatment*
Flux	0.71	0.99	1.12	1.39	**0.004**	**0.06**	0.63
(ugC g^{-1} h^{-1})	±0.14	±0.35	±0.41	±0.62			
qCO$_2$	1.09	1.15	1.51	1.81	**0.002**	0.21	0.67
(ugC gMBC h^{-1})	±0.3	±0.23	±0.55	±0.59			

Fig. 5. Enzyme activities in nmol g^{-1} h^{-1} in bulk and rhizosphere soils in function of treatments. Error bars represent standard error between replicates (n = 9). LAP = leucine amino-peptidase, BG = B-glucosidase, NAG = 1,4-N-acetyl-glucosaminidase, AP = acid phosphatase, PEROX = peroxidase, PHENOX = phenol oxidase. An asterisk indicates significant differences (p-value <0.05) between treatment for that soil fraction. Note the very different magnitudes of activity (i.e., y-axis ranges).

even a small addition of C in the bulk soil may trigger more changes than a larger addition in the rhizosphere, an already nutrient-rich environment. Thus, in our study, eCO$_2$ also influenced the bulk soil, giving it rhizosphere-like characteristics such as higher microbial biomass, respiration and N availability (Kuzyakov and Blagodatskaya, 2015). We cannot exclude the possibility of errors during the separation of bulk and rhizosphere soils where some rhizosphere soil might have fallen into the bulk soil, especially since rhizosphere soil can be attached more loosely to roots in organic soils compared to mineral soils. However, this potential error should have been consistent between eCO$_2$ and aCO$_2$.

Additionally, by increasing root biomass (Ziegler et al., 2023), eCO$_2$ likely expanded the proportion of rhizosphere soil as it was observed in our experiment (+2%) and to a larger extent at Duke FACE (Meier et al., 2015). Given that N mineralization is ten times faster in the rhizosphere, even a modest expansion of 2% in relative mass can potentially boost N gross mineralization by 18% when scaling-up to soil volume (2.53 µg N cm^{-3} d^{-1} under eCO$_2$ against 2.13 µg N cm^{-3} d^{-1} under aCO$_2$). Therefore, rhizosphere mass expansion might be a crucial mechanism for enhancing N availability that must not be disregarded when addressing tree N demand under future climates.

5. Conclusion

Collectively, our findings demonstrate that elevated CO$_2$ stimulates N cycling in the rhizosphere and bulk soils to meet microbial and tree N demand and reduce N losses in the rhizosphere, through a higher competition for available N. Our study proposes that the promotion of SOM decomposition and the control of N availability through plant and rhizobiome interactions could be a crucial mechanisms sustaining plant growth under higher atmospheric CO$_2$ concentrations. However, long-term studies need to track the trajectories of these processes to understand whether a shift may happen from abundant N supply to N limitation forcing long term C pool priming and leading to either a limitation of tree growth and/or a depletion of soil organic matter pool.

Funding

under elevated atmospheric CO2? (NE/T000449/1) and a Royal Society International Exchange grant (IES\R3\213025).

Appendix A. Supplementary data

Supplementary data to this article can be found online at https://doi.org/10.1016/j.soilbio.2024.109537.

References

Anderson, T., Domsch, K., 1993. The metabolic quotient for CO2 (qCO2) as a specific activity parameter to assess the effects of environmental conditions, such as ph, on the microbial biomass of forest soils. Soil Biology and Biochemistry 25, 393–395. https://doi.org/10.1016/0038-0717(93)90140-7.

Andresen, L.C., Carrillo, Y., Macdonald, C.A., Castañeda-Gómez, L., Bodé, S., Rütting, T., 2020. Nitrogen dynamics after two years of elevated CO2 in phosphorus limited Eucalyptus woodland. Biogeochemistry 150, 297–312. https://doi.org/10.1007/s10533-020-00699-y.

Barnard, R., Leadley, P.W., Hungate, B.A., 2005. Global change, nitrification, and denitrification: a review. Global Biogeochemical Cycles 19. https://doi.org/10.1029/2004GB002282.

Bates, D., Mächler, M., Bolker, B., Walker, S., 2015. Fitting linear mixed-effects models using **lme4**. Journal of Statistical Software 67. https://doi.org/10.18637/jss.v067.i01.

Brookes, P.C., Landman, A., Pruden, G., Jenkinson, D.S., 1985. Chloroform fumigation and the release of soil nitrogen: a rapid direct extraction method to measure microbial biomass nitrogen in soil. Soil Biology and Biochemistry 17, 837–842. https://doi.org/10.1016/0038-0717(85)90144-0.

Carney, K.M., Hungate, B.A., Drake, B.G., Megonigal, J.P., 2007. Altered soil microbial community at elevated CO2 leads to loss of soil carbon. Proceedings of the National Academy of Sciences 104, 4990–4995. https://doi.org/10.1073/pnas.0610045104.

Carrillo, Y., Dijkstra, F., LeCain, D., Blumenthal, D., Pendall, E., 2018. Elevated CO2 and warming cause interactive effects on soil carbon and shifts in carbon use by bacteria. Ecology Letters 21, 1639–1648. https://doi.org/10.1111/ele.13140.

Carrillo, Y., Dijkstra, F.A., Pendall, E., LeCain, D., Tucker, C., 2014. Plant rhizosphere influence on microbial C metabolism: the role of elevated CO2, N availability and root stoichiometry. Biogeochemistry 117, 229–240. https://doi.org/10.1007/s10533-014-9954-5.

Craine, J.M., Morrow, C., Fierer, N., 2007. Microbial nitrogen limitation increases decomposition. Ecology 88, 2105–2113. https://doi.org/10.1890/06-1847.1.

Davidson, E.A., Hart, S.C., Shanks, C.A., Firestone, M.K., 1991. Measuring gross nitrogen mineralization, and nitrification by 15 N isotopic pool dilution in intact soil cores. Journal of Soil Science 42, 335–349. https://doi.org/10.1111/j.1365-2389.1991.tb00413.x.

De Graff, M.-A., Van Groenigen, K.-J., Six, J., Hungate, B., Van Kessel, C., 2006. Interactions between plant growth and soil nutrient cycling under elevated CO2 : a meta-analysis. Global Change Biology 12, 2077–2091. https://doi.org/10.1111/j.1365-2486.2006.01240.x.

Dijkstra, F.A., Carrillo, Y., Pendall, E., Morgan, J.A., 2013. Rhizosphere priming: a nutrient perspective. Frontiers in Microbiology 4. https://doi.org/10.3389/fmicb.2013.00216.

Dong, J., Hunt, J., Delhaize, E., Zheng, S.J., Jin, C.W., Tang, C., 2021. Impacts of elevated CO2 on plant resistance to nutrient deficiency and toxic ions via root exudates: a review. Science of the Total Environment 754, 142434. https://doi.org/10.1016/j.scitotenv.2020.142434.

Dorodnikov, M., Kuzyakov, Y., Fangmeier, A., Wiesenberg, G.L.B., 2011. C and N in soil organic matter density fractions under elevated atmospheric CO2: turnover vs. stabilization. Soil Biology and Biochemistry 43, 579–589. https://doi.org/10.1016/j.soilbio.2010.11.026.

Fender, A.-C., Leuschner, C., Schützenmeister, K., Gansert, D., Jungkunst, H.F., 2013. Rhizosphere effects of tree species – Large reduction of N2O emission by saplings of ash, but not of beech, in temperate forest soil. European Journal of Soil Biology 54, 7–15. https://doi.org/10.1016/j.ejsobi.2012.10.010.

Finzi, A.C., DeLucia, E.H., Hamilton, J.G., Richter, D.D., Schlesinger, W.H., 2002. The nitrogen budget of a pine forest under free air CO2 enrichment. Oecologia 132, 567–578. https://doi.org/10.1007/s00442-002-0996-3.

Finzi, A.C., Moore, D.J.P., DeLucia, E.H., Lichter, J., Hofmockel, K.S., Jackson, R.B., Kim, H.-S., Matamala, R., McCarthy, H.R., Oren, R., Pippen, J.S., Schlesinger, W.H., 2006a. Progressive nitrogen limitation of ecosystem processes under elevated CO2 in a warm-temperate forest. Ecology 87, 15–25. https://doi.org/10.1890/04-1748.

Finzi, A.C., Sinsabaugh, R.L., Long, T.M., Osgood, M.P., 2006b. Microbial community responses to atmospheric carbon dioxide enrichment in a warm-temperate forest. Ecosystems 9, 215–226. https://doi.org/10.1007/s10021-005-0078-6.

Gardner, A., Ellsworth, D.S., Crous, K.Y., Pritchard, J., MacKenzie, A.R., 2021. Is photosynthetic enhancement sustained through three years of elevated CO2 exposure in 175-year-old *Quercus robur*. Tree Physiology 42, 130–144. https://doi.org/10.1093/treephys/tpab090.

Gaudel, G., Xing, L., Raseduzzaman, M., Poudel, M., Dong, W., Hu, C., 2024. Soil microbes, carbon, nitrogen, and the carbon to nitrogen ratio indicate priming effects across terrestrial ecosystems. Journal of Soils and Sediments 24, 307–322. https://doi.org/10.1007/s11368-023-03609-5.

Guyonnet, J.P., Vautrin, F., Meiffren, G., Labois, C., Cantarel, A.A.M., Michalet, S., Comte, G., Haichar, F. el Z., 2017. The effects of plant nutritional strategy on soil microbial denitrification activity through rhizosphere primary metabolites. FEMS Microbiology Ecology 93. https://doi.org/10.1093/femsec/fix022.

Hart, K.M., Curioni, G., Blaen, P., Harper, N.J., Miles, P., Lewin, K.F., Nagy, J., Bannister, E.J., Cai, X.M., Thomas, R.M., Krause, S., Tausz, M., MacKenzie, A.R., 2020. Characteristics of free air carbon dioxide enrichment of a northern temperate mature forest. Global Change Biology 26, 1023–1037. https://doi.org/10.1111/gcb.14786.

Hart, S.C., Nason, G.E., Myrold, D.D., Perry, D.A., 1994. Dynamics of gross nitrogen transformations in an old-growth forest: the carbon connection. Ecology 75, 880–891. https://doi.org/10.2307/1939413.

Hasegawa, S., Ryan, M.H., Power, S.A., 2023. CO2 concentration and water availability alter the organic acid composition of root exudates in native Australian species. Plant and Soil 485, 507–524. https://doi.org/10.1007/s11104-022-05845-z.

Hedges, L.V., Gurevitch, J., Curtis, P.S., 1999. The meta-analysis of response ratios in experimental ecology. Ecology 80, 1150–1156. https://doi.org/10.1890/0012-9658 (1999)080[1150:TMAORR]2.0.CO, 2.

Hofmockel, K.S., Zak, D.R., Moran, K.K., Jastrow, J.D., 2011. Changes in forest soil organic matter pools after a decade of elevated CO2 and O3. Soil Biology and Biochemistry 43, 1518–1527. https://doi.org/10.1016/j.soilbio.2011.03.030.

Hollis, J., Jones, B., Ullah, S., MacKenzie, R., Hart, K., 2021. Soil profile pit at BIFoR-FACE, norbury junction. Staffordshire.

Hyvönen, R., Ågren, G.I., Linder, S., Persson, T., Cotrufo, M.F., Ekblad, A., Freeman, M., Grelle, A., Janssens, I.A., Jarvis, P.G., Kellomäki, S., Lindroth, A., Loustau, D., Lundmark, T., Norby, R.J., Oren, R., Pilegaard, K., Ryan, M.G., Sigurdsson, B.D., Strömgren, M., Van Oijen, M., Wallin, G., 2007. The likely impact of elevated [CO$_2$], nitrogen deposition, increased temperature and management on carbon sequestration in temperate and boreal forest ecosystems: a literature review. New Phytologist 173, 463–480. https://doi.org/10.1111/j.1469-8137.2007.01967.x.

Jiang, M., Medlyn, B.E., Drake, J.E., Duursma, R.A., Anderson, I.C., Barton, C.V.M., Boer, M.M., Carrillo, Y., Castañeda-Gómez, L., Collins, L., Crous, K.Y., De Kauwe, M. G., Dos Santos, B.M., Emmerson, K.M., Facey, S.L., Gherlenda, A.N., Gimeno, T.E., Hasegawa, S., Johnson, S.N., Kännaste, A., Macdonald, C.A., Mahmud, K., Moore, B. D., Nazaries, L., Nielsen, E.H.J., Nielsen, U.N., Noh, N.J., Ochoa-Hueso, R., Pathare, V.S., Pendall, E., Pihlblad, J., Piñeiro, J., Powell, J.R., Power, S. A., Reich, P.B., Renchon, A.A., Riegler, M., Rinnan, R., Rymer, P.D., Salomón, R.L., Singh, B.K., Smith, B., Tjoelker, M.G., Walker, J.K.M., Wujeska-Klause, A., Yang, J., Zaehle, S., Ellsworth, D.S., 2020. The fate of carbon in a mature forest under carbon dioxide enrichment. Nature 580, 227–231. https://doi.org/10.1038/s41586-020-2128-9.

Jilling, A., Keiluweit, M., Contosta, A.R., Frey, S., Schimel, J., Schnecker, J., Smith, R.G., Tiemann, L., Grandy, A.S., 2018. Minerals in the rhizosphere: overlooked mediators of soil nitrogen availability to plants and microbes. Biogeochemistry 139, 103–122. https://doi.org/10.1007/s10533-018-0459-5.

Johansson, E.M., Fransson, P.M.A., Finlay, R.D., Van Hees, P.A.W., 2009. Quantitative analysis of soluble exudates produced by ectomycorrhizal roots as a response to ambient and elevated CO2. Soil Biology and Biochemistry 41, 1111–1116. https://doi.org/10.1016/j.soilbio.2009.02.016.

Johnson, D.W., 2006. Progressive N limitation in forests: review and implications for long-term responses to elevated CO$_2$. Ecology 87, 64–75. https://doi.org/10.1890/04-1781.

Jones, D., 2002. Simple method to enable the high resolution determination of total free amino acids in soil solutions and soil extracts. Soil Biology and Biochemistry 34, 1893–1902. https://doi.org/10.1016/S0038-0717(02)00203-1.

Kuzyakov, Y., 2002. Review: factors affecting rhizosphere priming effects. Journal of Plant Nutrition and Soil Science 165, 382–396. https://doi.org/10.1002/1522-2624 (200208)165:4<382::AID-JPLN382>3.0.CO;2.

Kuzyakov, Y., Blagodatskaya, E., 2015. Microbial hotspots and hot moments in soil: concept & review. Soil Biology and Biochemistry 83, 184–199. https://doi.org/10.1016/j.soilbio.2015.01.025.

Kuzyakov, Y., Horwath, W.R., Dorodnikov, M., Blagodatskaya, E., 2019. Review and synthesis of the effects of elevated atmospheric CO2 on soil processes: No changes in pools, but increased fluxes and accelerated cycles. Soil Biology and Biochemistry 128, 66–78. https://doi.org/10.1016/j.soilbio.2018.10.005.

Li, Y., Chapman, S.J., Nicol, G.W., Yao, H., 2018. Nitrification and nitrifiers in acidic soils. Soil Biology and Biochemistry 116, 290–301. https://doi.org/10.1016/j.soilbio.2017.10.023.

Luo, Y., Su, B., Currie, W.S., Dukes, J.S., Finzi, A., Hartwig, U., Hungate, B., Mc Murtrie, R.E., Oren, R., Parton, W.J., Pataki, D.E., Shaw, M.R., Zak, D.R., Field, C.B., 2004. Progressive nitrogen limitation of ecosystem responses to rising atmospheric carbon dioxide. BioScience 54, 731. https://doi.org/10.1641/0006-3568(2004)054 [0731:PNLOER]2.0.CO, 2.

Manzoni, S., Chakrawal, A., Spohn, M., Lindahl, B.D., 2021. Modeling microbial adaptations to nutrient limitation during litter decomposition. Front. For. Glob. Change 4, 686945. https://doi.org/10.3389/ffgc.2021.686945.

Matsui, M., Fowler, J.H., Walling, L.L., 2006. Leucine aminopeptidases: diversity in structure and function. Biological Chemistry 387. https://doi.org/10.1515/BC.2006.191.

McMurtrie, R.E., Norby, R.J., Medlyn, B.E., Dewar, R.C., Pepper, D.A., Reich, P.B., Barton, C.V.M., 2008. Why is plant-growth response to elevated CO2 amplified when water is limiting, but reduced when nitrogen is limiting? A growth-optimisation hypothesis. Functional Plant Biology 35, 521. https://doi.org/10.1071/FP08128.

Meier, I.C., Pritchard, S.G., Brzostek, E.R., McCormack, M.L., Phillips, R.P., 2015. The rhizosphere and hyphosphere differ in their impacts on carbon and nitrogen cycling in forests exposed to elevated CO$_2$. New Phytologist 205, 1164–1174. https://doi.org/10.1111/nph.13122.

Micucci, G., Sgouridis, F., McNamara, N.P., Krause, S., Lynch, I., Roos, F., Pereira, M.G., Ullah, S., 2024. Towards enhanced sensitivity of the 15N gas flux method for quantifying denitrification in soil. Soil Biology and Biochemistry 109421. https://doi.org/10.1016/j.soilbio.2024.109421.

Moorhead, D.L., Rinkes, Z.L., Sinsabaugh, R.L., Weintraub, M.N., 2013. Dynamic relationships between microbial biomass, respiration, inorganic nutrients and enzyme activities: informing enzyme-based decomposition models. Frontiers in Microbiology 4. https://doi.org/10.3389/fmicb.2013.00223.

Norby, R.J., Hanson, P.J., O'Neill, E.G., Tschaplinski, T.J., Weltzin, J.F., Hansen, R.A., Cheng, W., Wullschleger, S.D., Gunderson, C.A., Edwards, N.T., Johnson, D.W., 2002. Net primary productivity of a CO$_2$-enriched deciduous forest and the implications for carbon storage. Ecological Applications 12, 1261–1266. https://doi.org/10.1890/1051-0761(2002)012[1261:NPPOAC]2.0.CO;2.

Norby, R.J., Warren, J.M., Iversen, C.M., Medlyn, B.E., McMurtrie, R.E., 2010. CO2 enhancement of forest productivity constrained by limited nitrogen availability. Proceedings of the National Academy of Sciences 107, 19368–19373. https://doi.org/10.1073/pnas.1006463107.

Norby, R.J., Wullschleger, S.D., Gunderson, C.A., Johnson, D.W., Ceulemans, R., 1999. Tree responses to rising CO$_2$ in field experiments: implications for the future forest. Plant, Cell and Environment 22, 683–714. https://doi.org/10.1046/j.1365-3040.1999.00391.x.

Norby, R.J., Zak, D.R., 2011. Ecological Lessons from Free-Air CO2 Enrichment (FACE) Experiments.

Pellitier, P.T., Ibáñez, I., Zak, D.R., Argiroff, W.A., Acharya, K., 2021. Ectomycorrhizal access to organic nitrogen mediates CO2 fertilization response in a dominant temperate tree. Nature Communications 12, 5403. https://doi.org/10.1038/s41467-021-25652-x.

Philippot, L., Hallin, S., Börjesson, G., Baggs, E.M., 2009. Biochemical cycling in the rhizosphere having an impact on global change. Plant and Soil 321, 61–81. https://doi.org/10.1007/s11104-008-9796-9.

Phillips, R.P., Bernhardt, E.S., Schlesinger, W.H., 2009. Elevated CO2 increases root exudation from loblolly pine (Pinus taeda) seedlings as an N-mediated response. Tree Physiology 29, 1513–1523. https://doi.org/10.1093/treephys/tpp083.

Phillips, R.P., Finzi, A.C., Bernhardt, E.S., 2011. Enhanced root exudation induces microbial feedbacks to N cycling in a pine forest under long-term CO2 fumigation: rhizosphere feedbacks in CO2-enriched forests. Ecology Letters 14, 187–194. https://doi.org/10.1111/j.1461-0248.2010.01570.x.

Phillips, R.P., Meier, I.C., Bernhardt, E.S., Grandy, A.S., Wickings, K., Finzi, A.C., 2012. Roots and fungi accelerate carbon and nitrogen cycling in forests exposed to elevated CO$_2$. Ecology Letters 15, 1042–1049. https://doi.org/10.1111/j.1461-0248.2012.01827.x.

Pihlblad, J., Andresen, L.C., Macdonald, C.A., Ellsworth, D.S., Carrillo, Y., 2023. The influence of elevated CO$_2$ and soil depth on rhizosphere activity and nutrient availability in a mature *Eucalyptus* woodland. Biogeosciences 20, 505–521. https://doi.org/10.5194/bg-20-505-2023.

Rummel, P.S., Well, R., Pfeiffer, B., Dittert, K., Floßmann, S., Pausch, J., 2021. Nitrate uptake and carbon exudation – do plant roots stimulate or inhibit denitrification? Plant and Soil 459, 217–233. https://doi.org/10.1007/s11104-020-04750-7.

Rütting, T., Andresen, L.C., 2015. Nitrogen cycle responses to elevated CO2 depend on ecosystem nutrient status. Nutrient Cycling in Agroecosystems 101, 285–294. https://doi.org/10.1007/s10705-015-9683-8.

Schimel, J., Weintraub, M.N., Moorhead, D., 2022. Estimating microbial carbon use efficiency in soil: isotope-based and enzyme-based methods measure fundamentally different aspects of microbial resource use. Soil Biology and Biochemistry 169, 108677. https://doi.org/10.1016/j.soilbio.2022.108677.

Sgouridis, F., Reay, M., Cotchim, S., Ma, J., Radu, A., Ullah, S., 2023. Stimulation of soil gross nitrogen transformations and nitrous oxide emission under Free air CO2 enrichment in a mature temperate oak forest at BIFoR-FACE. Soil Biology and Biochemistry 184, 109072. https://doi.org/10.1016/j.soilbio.2023.109072.

Sinsabaugh, R.L., 2010. Phenol oxidase, peroxidase and organic matter dynamics of soil. Soil Biology and Biochemistry 42, 391–404. https://doi.org/10.1016/j.soilbio.2009.10.014.

Sinsabaugh, R.L., Turner, B.L., Talbot, J.M., Waring, B.G., Powers, J.S., Kuske, C.R., Moorhead, D.L., Follstad Shah, J.J., 2016. Stoichiometry of microbial carbon use efficiency in soils. Ecological Monographs 86, 172–189. https://doi.org/10.1890/15-2110.1.

Strauss, E.A., Lamberti, G.A., 2002. Effect of dissolved organic carbon quality on microbial decomposition and nitrification rates in stream sediments. Freshwater Biology 47, 65–74. https://doi.org/10.1046/j.1365-2427.2002.00776.x.

Stuart, E.K., Plett, K.L., 2020. Digging deeper: in search of the mechanisms of carbon and nitrogen exchange in ectomycorrhizal symbioses. Frontiers of Plant Science 10, 1658. https://doi.org/10.3389/fpls.2019.01658.

Subbarao, G.V., Rondon, M., Ito, O., Ishikawa, T., Rao, I.M., Nakahara, K., Lascano, C., Berry, W.L., 2007. Biological nitrification inhibition (BNI)—is it a widespread phenomenon? Plant and Soil 294, 5–18. https://doi.org/10.1007/s11104-006-9159-3.

Terrer, C., Phillips, R.P., Hungate, B.A., Rosende, J., Pett-Ridge, J., Craig, M.E., Van Groenigen, K.J., Keenan, T.F., Sulman, B.N., Stocker, B.D., Reich, P.B., Pellegrini, A. F.A., Pendall, E., Zhang, H., Evans, R.D., Carrillo, Y., Fisher, J.B., Van Sundert, K., Vicca, S., Jackson, R.B., 2021. A trade-off between plant and soil carbon storage under elevated CO2. Nature 591, 599–603. https://doi.org/10.1038/s41586-021-03306-8.

Terrer, C., Vicca, S., Stocker, B.D., Hungate, B.A., Phillips, R.P., Reich, P.B., Finzi, A.C., Prentice, I.C., 2018. Ecosystem responses to elevated CO$_2$ governed by plant–soil interactions and the cost of nitrogen acquisition. New Phytologist 217, 507–522. https://doi.org/10.1111/nph.14872.

U.S. DOE, 2020. U.S. Department of Energy Free-Air CO2 Enrichment Experiments: FACE Results, Lessons, and Legacy. U.S. Department of Energy Office of Science.

Van Groenigen, K.-J., de Graaff, M.-A., Six, J., Harris, D., Kuikman, P., van Kessel, C., 2006. The impact of elevated atmospheric [CO2] on soil C and N dynamics: a meta-analysis. In: Nösberger, J., Long, S.P., Norby, R.J., Stitt, M., Hendrey, G.R., Blum, H. (Eds.), Managed Ecosystems and CO2, Ecological Studies. Springer, Berlin Heidelberg, Berlin, Heidelberg, pp. 373–391. https://doi.org/10.1007/3-540-31237-4_21.

Verchot, L.V., Holmes, Z., Mulon, L., Groffman, P.M., Lovett, G.M., 2001. Gross vs net rates of N mineralization and nitrification as indicators of functional differences

between forest types. Soil Biology and Biochemistry 33, 1889–1901. https://doi.org/10.1016/S0038-0717(01)00095-5.

Xiao, W., Chen, X., Jing, X., Zhu, B., 2018. A meta-analysis of soil extracellular enzyme activities in response to global change. Soil Biology and Biochemistry 123, 21–32. https://doi.org/10.1016/j.soilbio.2018.05.001.

Yin, L., Dijkstra, F.A., Phillips, R.P., Zhu, B., Wang, P., Cheng, W., 2021. Arbuscular mycorrhizal trees cause a higher carbon to nitrogen ratio of soil organic matter decomposition via rhizosphere priming than ectomycorrhizal trees. Soil Biology and Biochemistry 157, 108246. https://doi.org/10.1016/j.soilbio.2021.108246.

Zhang, Y., Wang, J., Dai, S., Zhao, J., Huang, X., Sun, Y., Chen, J., Cai, Z., Zhang, J., 2019. The effect of C:N ratio on heterotrophic nitrification in acidic soils. Soil

Biology and Biochemistry 137, 107562. https://doi.org/10.1016/j.soilbio.2019.107562.

Zhu, X., Liu, D., Yin, H., 2021. Roots regulate microbial N processes to achieve an efficient NH4+ supply in the rhizosphere of alpine coniferous forests. Biogeochemistry 155, 39–57. https://doi.org/10.1007/s10533-021-00811-w.

Ziegler, C., Kulawska, A., Kourmouli, A., Hamilton, L., Shi, Z., MacKenzie, A.R., Dyson, R.J., Johnston, I.G., 2023. Quantification and uncertainty of root growth stimulation by elevated CO2 in a mature temperate deciduous forest. Science of the Total Environment 854, 158661. https://doi.org/10.1016/j.scitotenv.2022.158661.